Journal of Organometallic Chemistry, 284 (1985) 13–23
Elsevier Sequoia S.A., Lausanne – Printed in The Netherlands

SYNTHESIS AND X-RAY CRYSTALLOGRAPHIC CHARACTERIZATION OF $(\mu_3\text{-Bi})_2Fe_3(CO)_9$: A REFORMULATION OF HIEBER'S $Bi_2Fe_5(CO)_{20}$

MELVYN ROWEN CHURCHILL, JAMES C. FETTINGER,

Department of Chemistry, State University of New York at Buffalo, Buffalo, NY 14214 (U.S.A.)

and KENTON H. WHITMIRE

Department of Chemistry, Rice University, P.O. Box 1892, Houston, TX 77251 (U.S.A.)

(Received August 27th, 1984)

Summary

When $[HFe(CO)_4]^-$ is treated first with $NaBiO_3$ and then dilute H_2SO_4, a complex mixture of neutral metal carbonyl clusters results, some of which can be extracted into petroleum ether. Upon prolonged standing the extract yields a precipitate which has been characterized by X-ray crystallography as $Bi_2Fe_3(CO)_9$.

The complex $Bi_2Fe_3(CO)_9$ crystallizes in the centrosymmetric orthorhombic space group *Cmcm* (D_{2h}^{17}; No. 63) with a 10.616(2) Å, b 13.458(3) Å, c 11.347(3) Å, V 1621.1(7) Å^3 and $Z = 4$. Single-crystal X-ray diffraction data (Mo-K_α, $2\theta = 4.5$–$55.0°$) were collected on a Syntex $P2_1$ four-circle diffractometer and the structure was refined to R_F 5.4% and R_{wF} 4.5% for all 1039 independent data (R_F 4.5% and R_{wF} 4.5% for those 851 reflections with $|F_0| > 3.0\sigma(|F_0|)$). The molecule lies on a site of crystallographic C_{2v} symmetry and is disordered. The individual molecules have a trigonal bipyramidal Bi_2Fe_3 core with the bismuth atoms occupying the apical sites (Bi–Fe 2.617(2)–2.643(2) Å, Fe–Fe 2.735(5)–2.757(5) Å). Each iron atom is linked to three terminal carbonyl ligands and the molecule has approximate C_{3h} symmetry. The nine peripheral oxygen atoms are ordered and define a tricapped trigonal prism. The equatorial iron atoms are disordered with the two Fe_3 triangles mutually displaced by approximately 30°; the disordered ensemble has approximate D_{3h} symmetry.

Introduction

In 1959, Hieber and co-workers [1] reported the synthesis of an unusual bismuth-containing iron carbonyl cluster, which was formulated as $Bi_2Fe_5(CO)_{20}$ based on its elemental analyses and magnetic susceptibility. The structural possibilities for this cluster were intriguing in light of recent reports for other bismuth-containing metal

0022-328X/85/$03.30

carbonyls: $Bi[Co(CO)_4]_3$ [2], $BiIr_3(CO)_9$ [3], and $Bi_2[W(CO)_5]_3$ [4]. The cobalt complex adopts an open structure (no Co–Co bonds) while the iridium species is a *closo* tetrahedron. The fact that cobalt did not form Co–Co bonds was attributed to the steric requirements of the bismuth atom. We have shown recently, by a crystallographic analysis of $[(\mu_3\text{-Bi})Fe_3(CO)_9(\mu_3\text{-CO})]^-$ [5], that a first row transition metal carbonyl can form *closo* clusters incorporating bismuth. This molecule shows strain on the metal–metal framework in that the Fe–Fe bond lengths are comparable to the Fe–Bi distances. In $Bi_2[W(CO)_5]_3$ a short bismuth–bismuth distance indicates a bonding interaction, whereas the W–W distances are nonbonding. For these reasons it was of interest to undertake a crystallographic study of the material Hieber reported as $Bi_2Fe_5(CO)_{20}$. We wish to report here the structure of that product, which is now shown to be $Bi_2Fe_3(CO)_9$ (I).

Experimental

All manipulations were performed under an inert atmosphere of N_2 using standard Schlenk and vacuum line techniques. Solvents were dried by methods appropriate to each and deoxygenated. The water used was deionized and was bubbled with N_2 prior to use.

Synthesis of $Bi_2Fe_3(CO)_9$. Pentacarbonyliron (1.75 ml) is quickly syringed into cooled (ice bath) methanolic KOH (2.6 g in 15 ml) producing $[HFe(CO)_4]^-$. A slurry of $NaBiO_3$ (1.49 g) in H_2O (75 ml) is prepared in a dropping funnel attached to the iron carbonyl solution. The slurry is constantly bubbled with N_2 while being added dropwise to the methanol solution. The solution becomes dark and eventually green as addition progresses. The resultant solution is stirred for ca. 0.5 h longer. A dilute solution of H_2SO_4 is then added dropwise over a period of one to 2 h. The solution becomes brown shortly after addition begins and a black precipitate develops. The precipitate is collected by filtration, washed with H_2O and dried under vacuum. (The filtrate may be faint pink due to the formation of small amounts of $[HFe_3(CO)_{11}]^-$ which can be isolated as its Et_4N^+ salt and identified by infrared spectroscopy.) The dark solid is then extracted into petroleum ether (b.p. ~ 20–40°C; three times, 300 ml each) and the brown extracts are filtered, combined and allowed to stand under nitrogen for several weeks. During this time a dark precipitate develops. The residue after extraction still contains several unknown iron carbonyls some of which can be extracted into toluene and others which can be dissolved in acetone. The infrared spectra of all these extracts are highly variable and change with time indicating conversion to other species. The toluene solution also develops a precipitate, but none is seen for the acetone extracts. The precipitate from the petroleum ether solution, obtained in 7% yield, is soluble in acetone and gives a simple infrared spectrum (ν(CO) 2000s, 1963m cm^{-1}) which is identical to the infrared obtained for crystals grown from a toluene solution of the petroleum ether extracted material. The crystals for X-ray analysis were grown from a toluene solution of the petroleum ether extract.

Collection of the X-ray diffraction data

The crystal chosen for the diffraction study was a rectangular parallelepiped with approximate dimensions $0.2 \times 0.2 \times 0.3$ mm^3. It was sealed into a thin glass capillary

TABLE 1

EXPERIMENTAL DATA FOR THE X-RAY DIFFRACTION STUDY OF $Bi_2Fe_3(CO)_9$

(A) Crystallographic parameters at 24°C (297 K)

Crystal system: orthorhombic
a 10.6159(24) Å
b 13.4582(33) Å
c 11.3469(35) Å
V 1621.1(7) $Å^3$

Space group: *Cmcm* (D_{2h}^{17}; No. 63)
Formula: $C_9O_9Bi_2Fe_3$
mol. wt.: 837.60
$Z = 4$
D(calc'd) 3.43 g cm^{-3}

(B) Measurement of intensity data

Diffractometer: Syntex $P2_1$
Radiation: Mo-K_α ($\bar{\lambda}$ 0.710730 Å)
Monochromator: pyrolytic graphite ($2\theta_m = 12.160°$ for 002 reflection), equatorial mode, assumed to be 50% perfectly/50% ideally mosaic for polarization correction.
Reflections measured: $+h$, $+k$, $\pm l$ for $2\theta = 4.5$–$55.0°$.
Scan type: coupled θ(crystal)-2θ(counter)
Scan width: symmetrical, $[1.8 + \Delta(\alpha_2 - \alpha_1)]°$
Background measurements: stationary crystal and stationary counter at beginning and end of 2θ scan, each for 50% of total scan time.
Standard reflections: 3 mutually orthogonal reflections recollected after every 47 data; no decay observed.
Total measurements: 2191 total; merged to 1039 unique data after correction for absorption ($R(I)$ 4.33%, $R(wI)$ 4.82%) (Churchill's local file name CMCM).
Absorption coefficient: μ 233.0 cm^{-1}; all data corrected empirically by interpolation (in ϕ and 2θ) between three close-to-axial ψ-scans.

---

under an inert atmosphere and was mounted into a eucentric goniometer on the Syntex $P2_1$ automated four-circle diffractometer at SUNY-Buffalo. All subsequent set-up operations (i.e., determination of the crystal's unit cell dimensions and orientation matrix) and data collection (Mo-K_α radiation; coupled θ(crystal)–2θ(counter) scan technique) were performed as has been described previously [6]. Details of the present study are provided in Table 1.

The systematic absences (*hkl* for $h + k = 2n + 1$ and *h0l* for $l = 2n + 1$) are consistent with either the noncentrosymmetric orthorhombic space group $Cmc2_1$ (C_{2v}^{12}; No. 36) [7a] or the centrosymmetric orthorhombic space group *Cmcm* (D_{2h}^{17}; No. 63) [7b]. With only four molecules per unit cell, the crystallographic asymmetric unit is one-half of the $Bi_2Fe_3(CO)_9$ molecule in space group $Cmc2_1$ or one-fourth of the $Bi_2Fe_3(CO)_9$ molecule in space group *Cmcm*. Because of the likelihood of the non-centrosymmetric space group we elected to collect two octants of data ($+h$, $+k$, $\pm l$).

Diffraction data were corrected for absorption (via interpolation in ϕ and 2θ between a set of ψ-scans of close-to-axial reflections) and for Lorentz and polarization effects. All data were reduced to unscaled $|F_0|$ values, any reflection with $I(\text{net}) < 0$ being assigned an $|F_0|$ value of zero.

Determination of the crystal structure

All crystallographic calculations were performed on our in-house Syntex XTL system consisting of a Data General NOVA 1200 computer (with parallel floating-point processor), a Diablo disk unit, a Versatec printer/plotter and the SUNY-Buffalo modified version of the XTL interactive crystallographic program package.

The analytical form of the scattering factor for the appropriate neutral atoms [8a] were used in calculating F_c values; these were corrected for both the real ($\Delta f'$) and imaginary ($\Delta f''$) components of anomalous dispersion [8b].

The analysis was begun under the assumption (later proved to be erroneous) that the crystal belonged to the non-centrosymmetric space group $Cmc2_1$. The position of the single crystallographically independent bismuth atom was located from an E-map based on the best MULTAN [9] solution. In space group $Cmc2_1$, the molecule lay on the mirror plane at $x = 0$. Subsequent difference-Fourier syntheses revealed all iron and oxygen atoms (and several carbon atoms) of a clearly disordered structure and indicated that the structure had C_{2v} ($mm2$) symmetry rather than C_s (m) symmetry; this corresponds to the centrosymmetric space group *Cmcm*. The analysis was continued in this higher space group; full-matrix least-squares refinement converged with [10] R_F 5.4%, R_{wF} 4.5% and GOF = 1.397 for all

TABLE 2

A. ATOMIC COORDINATES FOR $Bi_2Fe_3(CO)_9$

Atom	G[a]	x	y	z
Bi	1/2	0.19746(4)	0.24445(3)	1/4
Fe(1)	1/4	0	0.35759(18)	0.21369(29)
Fe(2)	1/4	0	0.15991(25)	0.15509(34)
Fe(3)	1/4	0	0.21427(25)	0.38733(34)
C(11)	1/4	0	0.3311(29)	0.0284(46)
C(11A)	1/4	0	0.3639(35)	0.0651(56)
C(12)[b]	1/2	0.1197(12)	0.4483(8)	1/4
C(21)[b]	1	0.1187(9)	0.1427(7)	0.0415(9)
C(22)	1/4	0	0.0415(15)	0.2240(20)
O(11)	1/2	0	0.3822(10)	−0.0414(11)
O(12)	1/2	0.1884(10)	0.5125(7)	1/4
O(21)	1	0.1873(7)	0.1134(7)	−0.0259(8)
O(22)	1/4	0	−0.0376(9)	1/4

B. ANISOTROPIC THERMAL PARAMETERS[c]

Atom	B_{11}	B_{22}	B_{33}	B_{12}	B_{13}	B_{23}
Bi	1.738(18)	2.330(19)	3.467(26)	0.148(14)	0	0
Fe(1)	1.88(11)	1.380(88)	2.98(20)	0	0	0.30(10)
Fe(2)	2.34(13)	1.87(11)	2.38(16)	0	0	−0.24(12)
Fe(3)	2.55(13)	1.84(11)	2.40(16)	0	0	−0.09(12)
C(11)	1.3(11)	6.1(21)	6.0(25)	0	0	4.1(19)
C(11A)	7.4(23)	4.8(21)	8.0(30)	0	0	−0.6(19)
C(12)	2.70(57)	2.16(44)	6.5(10)	0.37(39)	0	0
C(21)	3.88(43)	3.90(38)	2.82(44)	0.26(33)	−0.70(36)	−1.46(36)
C(22)	2.99(92)	2.81(79)	1.6(17)	0	0	−0.92(76)
O(11)	8.77(83)	5.99(59)	3.37(59)	0	0	1.44(57)
O(12)	4.81(53)	2.63(35)	10.5(11)	−1.71(38)	0	0
O(21)	6.36(45)	7.38(48)	5.04(45)	0.66(38)	2.87(37)	−1.12(44)
O(22)	5.88(86)	2.21(52)	6.7(11)	0	0	0

[a] "G" is the occupancy (for computing purposes). [b] This is probably a "composite atom" (see text). [c] The anisotropic thermal parameters enter the expression for the calculated structure factor in the form: $\exp[-0.25(h^2a^{\star 2}B_{11} + \ldots 2hka^{\star}b^{\star}B_{12} + \ldots)]$.

1039 independent reflections (none rejected) and R_F 4.3% and R_{wF} 4.3% for those 851 data with $|F_0| > 3.0\sigma(|F_0|)$.

The function minimized during the least-squares refinement was $\Sigma w(|F_0| - |F_c|)^2$ where $1/w = [\{\sigma(|F_0|)\}^2 + \{0.01|F_0|\}^2]$. A final difference-Fourier synthesis was "clean" indicating that the structure is both correct and complete. Final atomic positions and anisotropic thermal parameters (with esd's) are listed in Table 2.

Description of the molecular structure

Crystals consist of discrete molecules of $Bi_2Fe_3(CO)_9$ which lie on sites of crystallographic C_{2v} ($mm2$) symmetry. The structure is disordered with two possible orientations for each molecule (related by the mirror plane at $z = 1/4$). Figures 1 and 2 show the atomic labeling scheme, indicate the nature of the crystallographic disorder and depict the geometry of the isolated $Bi_2Fe_3(CO)_9$ molecule. Figure 3 provides a stereoscopic view of the disordered structure. Interatomic distances and angles are collected in Tables 3 and 4.

Each molecule contains a trigonal bipyramidal Bi_2Fe_3 core with the bismuth atoms in apical sites and the iron atoms in equatorial sites (at $x = 0$). Each iron atom is linked to three terminal carbonyl ligands, the molecule as a whole having approximate C_{3h} symmetry. The nine peripheral oxygen atoms are ordered and define a tricapped trigonal prism (of approximate D_{3h} symmetry). The equatorial iron atoms are disordered with the two Fe_3 triangles mutually displaced by about 31.3° (< Fe(1)...centr...Fe(1′) 30.28°, Fe(2)...centr...Fe(3′) 31.97°, and Fe(3)...centr...Fe(2′) 31.97°). The structure is completed by the carbon atoms of the carbonyl groups. In all probability there are 18 sites, each of half occupancy. However, it has been possible to resolve only three pairs of "half-carbon" atoms (C(22) and C(22′), C(11) and C(11A), and C(11′) and C(11A′)). These carbon atoms come from well-separated pairs of iron atoms (i.e., Fe(2)...Fe(2′) 2.154(6) Å, Fe(1)...Fe(3′) 2.244(4) Å and Fe(1′)...Fe(3) 2.244(4) Å. The other pairs of half-

(Continued on p. 20)

TABLE 3

INTERATOMIC DISTANCES (Å) FOR $Bi_2Fe_3(CO)_9$

(A) Metal – metal distances			
Bi–Fe(1)	2.623(2)	Fe(1)...Fe(1′)	0.824(5)
Bi–Fe(2)	2.617(2)	Fe(1)...Fe(3′)	2.244(4)
Bi–Fe(3)	2.643(2)	Fe(1′)...Fe(3)	2.244(4)
Fe(1)–Fe(2)	2.742(4)	Fe(2)...Fe(3′)	0.876(5)
Fe(1)–Fe(3)	2.757(5)	Fe(2′)...Fe(3)	0.876(5)
Fe(2)–Fe(3)	2.735(5)	Fe(2)...Fe(2′)	2.154(6)
(B) Iron – carbonyl distances			
Fe(1)–C(11A)	1.687(63)	C(11A)–O(11)	1.234(63)
Fe(1)–C(12)	1.809(12)	C(12)–O(12)	1.131(15)
Fe(1)–C(12″)	1.809(12)	C(12″)–O(12″)	1.131(15)
Fe(2)–C(21)	1.817(10)	C(21)–O(21)	1.127(13)
Fe(2)–C(21″)	1.817(10)	C(21″)–O(21″)	1.127(13)
Fe(2)–C(22)	1.774(21)	C(22)–O(22)	1.105(23)
Fe(3)–C(11′)	1.840(43)	C(11′)–O(11′)	1.048(47)
Fe(3)–C(21′)	1.780(10)	C(21′)–O(21′)	1.127(13)
Fe(3)–C(21‴)	1.780(10)	C(21‴)–O(21‴)	1.127(13)

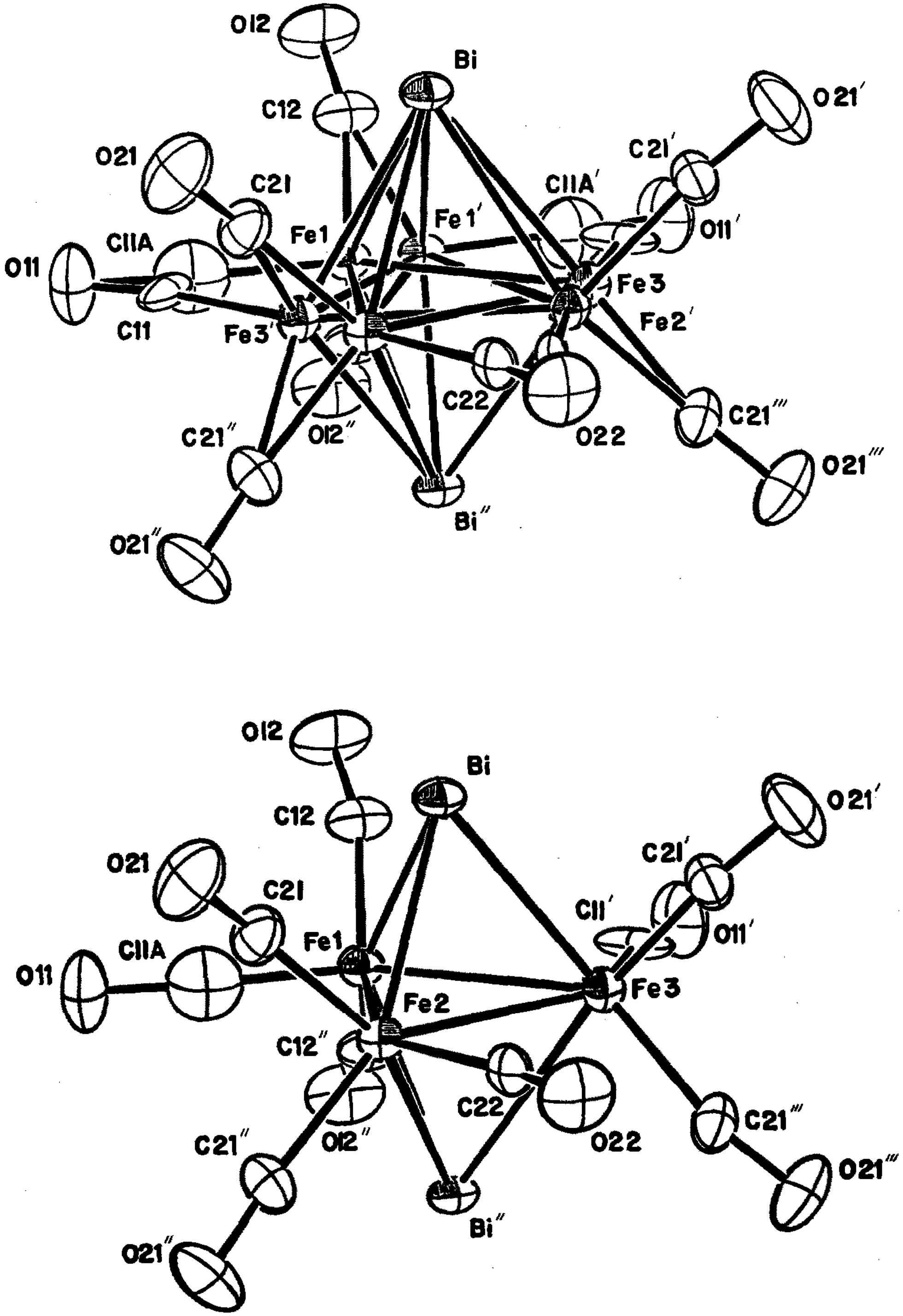

Fig. 1. General ORTEP-II view of $Bi_2Fe_3(CO)_9$. (a) The composite disordered structure. The unlabelled atom at the front of the molecule near Fe(3') is Fe(2). The label has been omitted due to the crowding in that area of the picture. (b) The isolated $Bi_2Fe_3(CO)_9$ molecule.

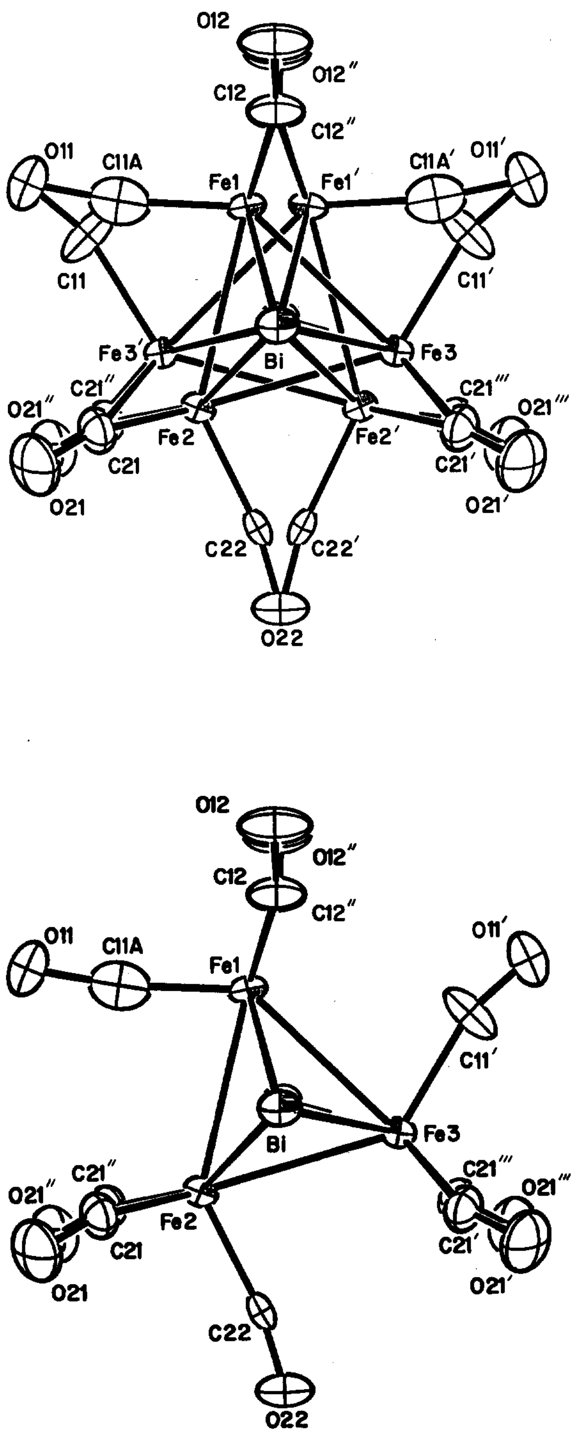

Fig. 2. Projection of the structure onto the equatorial plane (i.e., $x = 0$). (a) The composite disordered structure. (b) The isolated $Bi_2Fe_3(CO)_9$ molecule.

carbon atoms come from iron atoms that are much closer together and they have not been resolved. Thus both Fe(1) and Fe(1′) possess carbonyl ligands terminating at atom O(12). The separation Fe(1)...Fe(1′) = 0.824(5) Å, taken with idealized Fe–C and C–O distances of ~ 1.81 and ~ 1.13 Å, respectively, indicate that, with ideally linear Fe(1)–C–O(12) and Fe(1′)–C′–O(12) systems, the C...C′ separation would be ~ 0.32 Å (i.e., (0.824 × 1.13)/(1.81 + 1.13) Å; this is beyond the limits of resolution of the current study. Thus it is probable that C(12) (and its symmetry-related C(12″)) and C(21) (and the symmetry-related C(21′), C(21″) and C(21‴)) are all "composite atoms" derived from the sum of two half-carbon atoms separated by only about 0.3 Å. This should be borne in mind when considering distances and

TABLE 4

INTERATOMIC ANGLES (in deg.) FOR $Bi_2Fe_3(CO)_9$

(A) M–M–M Angles			
Fe(1)–Bi–Fe(2)	63.11(8)	Bi–Fe(2)–Fe(3)	59.15(9)
Fe(1)–Bi–Fe(3)	63.14(8)	Bi–Fe(2)–Fe(1)	58.56(8)
Fe(2)–Bi–Fe(3)	62.65(9)	Fe(1)–Fe(2)–Fe(3)	60.45(10)
Bi–Fe(1)–Bi″	106.08(8)	Bi–Fe(3)–Fe(1)	58.08(8)
Bi–Fe(2)–Bi″	106.45(10)	Bi–Fe(3)–Fe(2)	58.20(9)
Bi–Fe(3)–Bi″	104.94(10)	Fe(1)–Fe(3)–Fe(2)	59.91(10)
Fe(2)–Fe(1)–Fe(3)	59.64(10)	Fe(1)...centr...Fe(1′) [a]	30.28
Bi–Fe(1)–Fe(2)	58.33(8)	Fe(2)...centr...Fe(3′) [a]	31.97
Bi–Fe(1)–Fe(3)	58.78(8)	Fe(3)...centr...Fe(2′) [a]	31.97
(B) C–M–M Angles			
C(11A)–Fe(1)–Bi	100.7(15)	C(21)–Fe(2)–Bi	154.52(34)
C(11A)–Fe(1)–Fe(2)	78.9(15)	C(21)–Fe(2)–Fe(1)	107.20(33)
C(11A)–Fe(1)–Fe(3)	138.5(16)	C(21)–Fe(2)–Fe(3)	135.84(34)
C(12)–Fe(1)–Bi	78.16(32)	C(21″)–Fe(2)–Bi	77.98(32)
C(12)–Fe(1)–Fe(2)	135.21(34)	C(21″)–Fe(2)–Fe(1)	107.20(33)
C(12)–Fe(1)–Fe(3)	108.01(33)	C(21″)–Fe(2)–Fe(3)	135.84(34)
C(12″)–Fe(1)–Bi	156.47(34)	C(22)–Fe(2)–Bi	102.07(57)
C(12″)–Fe(1)–Fe(2)	135.21(34)	C(22)–Fe(2)–Fe(1)	139.83(58)
C(12″)–Fe(1)–Fe(3)	108.01(33)	C(22)–Fe(2)–Fe(3)	79.38(57)
C(11′)–Fe(3)–Bi	100.1(12)	C(21′)–Fe(3)–Fe(2)	106.99(34)
C(11′)–Fe(3)–Fe(1)	76.9(12)	C(21‴)–Fe(3)–Bi	155.79(35)
C(11′)–Fe(3)–Fe(2)	136.8(12)	C(21‴)–Fe(3)–Fe(1)	134.65(35)
C(21′)–Fe(3)–Bi	77.82(33)	C(21‴)–Fe(3)–Fe(2)	106.99(34)
C(21′)–Fe(3)–Fe(1)	134.65(35)		
(C) C–Fe–C Angles			
C(11A)–Fe(1)–C(12)	101.2(16)	C(21″)–Fe(2)–C(22)	101.4(7)
C(11A)–Fe(1)–C(12″)	101.2(16)	C(11′)–Fe(3)–C(21′)	103.1(12)
C(12)–Fe(1)–C(12″)	89.2(5)	C(11′)–Fe(3)–C(21‴)	103.1(12)
C(21)–Fe(2)–C(21″)	87.8(5)	C(21′)–Fe(3)–C(21‴)	90.2(5)
C(21)–Fe(2)–C(22)	101.4(7)		
(D) Fe–C–O Angles			
Fe(1)–C(11A)–O(11)	171.4(36)	Fe(2)–C(22)–O(22)	169.4(15)
Fe(1)–C(12)–O(12)	165.6(9)	Fe(3)–C(11′)–O(11′)	162.3(32)
Fe(1)–C(12″)–O(12″)	165.6(9)	Fe(3)–C(21′)–O(21′)	166.8(9)
Fe(2)–C(21)–O(21)	166.8(9)	Fe(3)–C(21‴)–O(21‴)	166.8(9)
Fe(2)–C(21″)–O(21″)	166.8(9)		

[a] "centr" is the mid-point of the Bi...Bi″ vector.

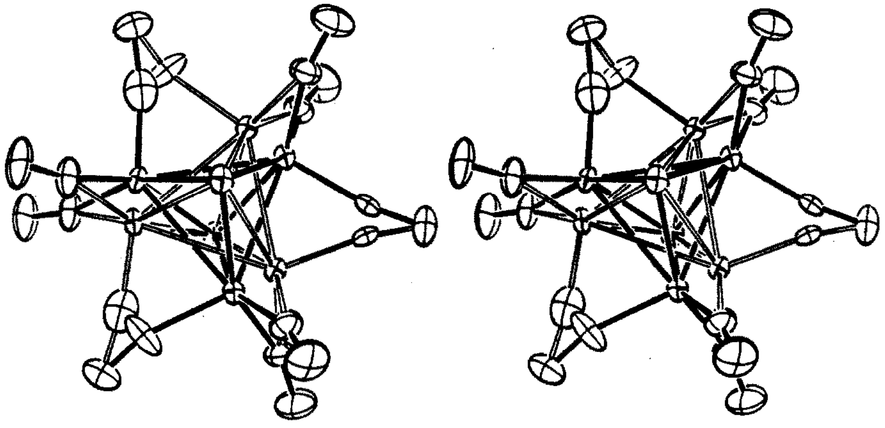

Fig. 3. Stereoscopic view of the entire disordered structure. One of the component molecules is linked by solids bonds, while the other is linked by hollow bonds (ORTEP-II diagram; 30% ellipsoids).

angles involving these carbon atoms; there are possible systematic errors inherent in these dimensions.

Within the $Bi_2Fe_3(CO)_9$ molecule, the iron–iron distances (Fe(1)–Fe(2) 2.742(4) Å, Fe(1)–Fe(3) 2.757(5) Å, Fe(2)–Fe(3) 2.735(5) Å; average 2.745{11} Å [11]) are substantially longer than the bismuth–iron distances (Bi–Fe(1) = Bi′–Fe(1) = 2.623(2) Å, Bi–Fe(2) = Bi′–Fe(2) = 2.617(2) Å, Bi–Fe(3) = Bi′–Fe(3) = 2.643(2) Å; average 2.628{14} Å). This is in contrast to our previous study [5] on the tetrahedral $BiFe_3$ species $[BiFe_3(CO)_9(\mu_3\text{-}CO)]^-$ in which the Fe–Fe distances were marginally shorter than the Bi–Fe distances (viz., 2.642(7) Å vs. 2.650(2) Å). Since the core structures are very similar (cf. I and II, below), it follows that (as might be expected) Fe–Fe distances within the Fe_3 triangle are contracted more by the μ_3-CO ligand than by a μ_3-Bi atom.

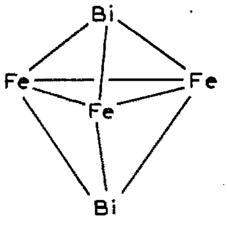

(I)

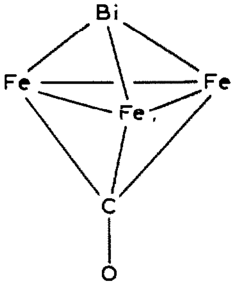

(II)

Each $Fe(CO)_3$ group appears to have only C_s (rather than C_{3v}) symmetry, with two large and one small C–Fe–C angle. Thus, around Fe(1), we have C(11A)–Fe(1)–C(12) = C(11A)–Fe(1)–C(12″) = 101.2(16)° vs. C(12)–Fe(1)–C(12″) 89.2(5)°. Similar variations occur around Fe(2) (101.4(7)° twice and 87.8(5)°) and

Fe(3) (103.1(12)° twice and 90.2(5)°) and are to be expected since the symmetry of the iron atom's environment is lower than C_{3v} (see ref. 12); the magnitude of the variations may be overestimated because of the probable "composite" nature of all non-equatorial carbonyl carbon atoms.

Discussion

Hieber and co-workers reported that protonation of solutions formed by treating $Fe(CO)_5$ with base and then sodium bismuthate yielded a neutral bismuth-containing cluster formulated as $Bi_2Fe_5(CO)_{20}$. Repeating this work in order to obtain some of the material for structural analysis has led to several conclusions. First, the material obtained upon protonation appears to be a complex mixture of metal carbonyls as determined by infrared spectroscopy. Only a small fraction of this material is soluble in petroleum ether and IR spectra indicate that the products are unstable. In the case of the petroleum ether extract, a solid slowly precipitates from solutions (as reported by Hieber), which we have determined by X-ray crystallography to be $Bi_2Fe_3(CO)_9$ and not $Bi_2Fe_5(CO)_{20}$ as previously suggested. The infrared spectra of the initial solutions give no evidence of I. Evidently, unstable species are produced on protonation which decompose to give the title compound in low yield (ca. 7%). Similar results have been obtained for protonation of $Ru_3(CO)_{12}$ after treatment with XO_3^{2-} (X = S, Se, Te) in alkaline medium [13]. In that case, however, the hydrido clusters $H_2Ru_3(CO)_9X$ were obtained. It is likely that for all these systems initial attack of the oxo species occurs at CO to liberate CO_2 and form metal carbonyl anions which are then protonated [5]. A difference between the bismuth and Group VI systems is that this protonation does not result in the isolation of a hydrido species as it does for X = S, Se, Te. The various species which decompose to $Bi_2Fe_3(CO)_9$ may be unstable hydride intermediates.

The structure of I is interesting because of the steric demand placed on the cluster framework by the size of the two bismuth atoms. The strain is evidenced by the fact that the Fe–Fe distances are longer than the Fe–Bi distances (2.745(11) Å vs. 2.628(14) Å). It represents only the second *closo*-cluster of the first transition series which contains bismuth. The other is $[(\mu_3\text{-Bi})Fe_3(CO)_9(\mu_3\text{-CO})]^-$ (II) which we have recently reported and with which I is isoelectronic. An arsenic analogue, $Fe_3As_2(CO)_9$, is known [14], but the smaller size of arsenic places little strain on the metal framework as evidenced by the shorter (by ca. 0.12 Å) Fe–Fe distances. These distances can be compared to those observed for other simple iron carbonyls: $[Fe_4(CO)_{13}]^{2-}$ (2.54 Å, ave), [15] $[Fe_3(CO)_{11}]^{2-}$ (2.60 Å, ave) [16] and $Fe_3(CO)_{12}$ (2.64 Å, ave) [17]. The exceptionally long Fe–Fe distance in $[Fe_2(CO)_8]^{2-}$ (2.79 Å) [18] is comparable to that observed for I but is thought to arise for electronic rather than steric reasons. The analogous cobalt system has only been observed to form complexes with Bi in which there are no Co–Co bonds, supposedly because of the steric demand of Bi [2]. In $[(\mu_3\text{-Bi})Fe_3(CO)_9(\mu_3\text{-CO})]^-$ the lengthening effect of bismuth may be counterbalanced by a shortening imposed by the μ_3-CO, since the Fe–Fe bonds (2.642(7) Å) are shorter than seen for I.

With the characterization of this molecule there are now available two extremes in the bonding of these cluster-types. Here, there is no Bi–Bi bond, but bonding is evidenced between the iron carbonyl units. At the other extreme is $Bi_2[W(CO)_5]_3$ in which there is a Bi–Bi interaction but no W–W bonds are formed.

Supplementary material available

A list of observed and calculated structure factor amplitudes is available upon request from Melvyn R. Churchill.

Acknowledgments

This work was supported, in part, by NSF Grant CHE80-23448 (to M.R.C.), and by the Petroleum Research Fund administered by the American Chemical Society and the Robert A. Welch Foundation (to K.H.W.).

References

1 W. Hieber, J. Gruber and F. Lux, Z. Anorg. Allg. Chem., 300 (1959) 275.

2 G. Etzrodt, R. Boese and G. Schmid, Chem. Ber., 112 (1979) 2574.

3 W. Kruppa, D. Bläser, R. Boese and G. Schmid, Z. Naturforsch. B, 37 (1982) 209.

4 G. Huttner, U. Weber and L. Zsolnai, Z. Naturforsch. B, 37 (1982) 707.

5 K.H. Whitmire, C.B. Lagrone, M.R. Churchill, J.C. Fettinger and L.V. Biondi, Inorg. Chem., 23 (1984) in press.

6 M.R. Churchill, R.A. Lashewycz and F.J. Rotella, Inorg. Chem., 16 (1977) 265.

7 International Tables for X-Ray Crystallography, Volume I, Kynoch Press, Birmingham, England, 1965, (a) p. 122; (b) p. 152.

8 International Tables for X-Ray Crystallography, Volume IV, Kynoch Press, Birmingham, England, 1974, (a) p. 99–101; (b) pp. 149–150.

9 G. Germain, P. Main and M.M. Woolfson, Acta Crystallogr., Section A, 27 (1971) 368.

10 $R_F(\%) = 100(\Sigma||F_0| - |F_c||)/\Sigma|F_0|$; $R_{wF}(\%) = 100[\Sigma w(|F_0| - |F_c|)^2/\Sigma w/F_0|^2]^{1/2}$; GOF $= [\Sigma w(|F_0| - |F_c|)^2/(\text{NO} - \text{NV})]^{1/2}$, where NO is number of observations and NV is number of variables.

11 Esd's of average values, shown in curly brackets, are calculated by the scatter formula:

$$\{\sigma\} = \left[\sum_N (d_i - \bar{d})^2/(N-1)\right]^{1/2}.$$

Here $\bar{d}$ is the average of N equivalent measurements and d_i is the ith such measurement.

12 S.F.A. Kettle, Inorg. Chem., 4 (1965) 1661.

13 E. Sappa, O. Gambino and G. Cetini, J. Organomet. Chem., 35 (1972) 375.

14 L.T.J. Delbaere, L.J. Kruczynski and D.W. McBride, J. Chem. Soc., Dalton Trans., (1973) 307.

15 R.J. Doedens and L.F. Dahl, J. Am. Chem. Soc., 88 (1966) 4847.

16 F.Y.-K. Lo, G. Longoni, P. Chini, L.D. Lower and L.F. Dahl, J. Am. Chem. Soc., 102 (1980) 7691.

17 F.A. Cotton and J.M. Troup, J. Am. Chem. Soc., 96 (1974) 4155.

18 H.B. Chin, M.B. Smith, R.D. Wilson and R. Bau, J. Am. Chem. Soc., 96 (1974) 5285.